Experiments on Crack Opening and Leak Rate Behaviour of Small Piping Components at the HDR Facility

H. HUNGER, G. KATZENMEIER
Kernforschungszentrum, Karlsruhe, FRG
H. GREBNER
Gesellschaft fur Reaktorsicherheit, Köln, FRG

ABSTRACT

Experiments were carried out on small bore austenitic piping components (under DN100) at the HDR (hot steam reactor) test installation for the purpose of examining crack opening and fluid discharge (leak) behaviour. The pipes at elevated internal pressure and temperature were, in addition, subjected to externally applied bending moments. The applied load, the resulting temperatures, strains, crack opening and fluid leak rates were measured. A few representive measurements on straight pipes (DN80) with circumferential flaws were selected and are presented here.

1 INTRODUCTION

Since 1988, six pipe leak experiments supervised by the Nuclear Research Centre in Karlsruhe (Project HDR Safety Program, PHDR, Phase III), have been carried out at the HDR plant, under the auspices of German research into nuclear safety (BMFT). Four austenitic pipes (DN80) with circumferential cracks and two nozzle/pipe attachments (DN25/100), also austenite, with cracks in the weldments were examined. The tests were carried out under simulated pressure water reactor conditions (T = 308°C, p = 10,8 MPa). The object of the tests was to determine the rate of leakage under constant internal pressure with a stepwise increasing or decreasing bending moment, which effects an opening or closing of the crack resp. It should thus be avoided that false conclusions be drawn in practice about the rate of leakage through a crack of unknown size. This is especially important for small bore pipes of up to DN200, where most leaks occur in practice.

2 TEST RIG

The individual test pipes were provided with pressurized water through a pipe (DN80) connected to the pressure vessel of the HDR, capacity 75 m^3 (see Fig. 1). By opening both valves, hot

SMiRT 11 Transactions Vol. F (August 1991) Tokyo, Japan, © 1991

water was allowed to flow through and thus heat up the test pipe. After a few minutes the valve in the small bore heating pipe (DN25) was closed, thus creating the situation that the water flowing in the feed pipe could only escape through the flaw i.e. the mass flow rate measured in the feed pipe was the same as the leak rate through the crack. The rigs for the tests on nozzles (DN25) welded onto pipes (DN100) with simulated flaws of 90°and 180° in the weld resp. are simular (tests E22.11 and E22.12). These latter tests are not dealt with here. Each artificially flawed test specimen is welded into and near the end of a pipe which is clamped at this end and forms a cantilever of 1,5 - 2,0 m length. The pipe is subjected to bending moments which are produced with a displacement controlled hydraulic cylinder attached at the free end of the cantilever. The circumferential flaws for the tests introduced here, E22.01 to E22.05 are collectively described in fig. 2. Involved are erosive produced slits or genuine cracks of lengths between 30°and 90°, produced through fatigue tests in the laboratory.

Two test pipes were examined in each test phase, whereby 50-60 measuring devices were employed for each phase. The pressure, temperatures at inside and outside of pipewall and strains are to be measured at strategic locations. The applied load and pipe deflection at the hydraulic attachment, crack opening (CMOD) and the rate of leakage - this last fourfold redundant - are also to be measured.

3 TEST RESULTS

The "cold" test E22.03 (without pressure and water) allows the relationship between the pre-selected positive zylinder travel, the resulting force and finally, the increasing crack opening to be clearly demonstrated (Fig. 3); the cracks for E22.02 and E22.03 are identical. The clear relationships between these variables for actual leaks at the elevated temperatures and pressures is unfortunately superposed with extraneous influences, presumably due to temperature effects. The following curves show this.

The tests E22.02 and E22.04 were chosen for this purpose. Fig. 4 shows the lateral deflection of the pipe and the force exerted on the pipe by the movement controlled hydraulic cylinder. As for all tests, the crack was opened and closed several times corresponding to the stepwise variations in load (bending moment). The measured load is not quite proportional to the lateral pipe deflection, deviations being due to transients, which are probably temperature effects. Fig. 5 shows the associated leakrates (measured with a blender and with the correlation procedure) and the temperature of the feed water as a function of time. The time range from 0-200 s is the heating-up phase of the test pipe. The leakage rate through the 28° crack hardly changes, remaining under 0,3 kg/s.

The crack for E22.04 Part I has a length of 50°. Fig. 6 shows again the lateral load on the pipe and travel of the hydraulic cylinder. This test begins with a negative travel i.e. with the crack pressed together. The time range from 0-600 s served as the heating-up phase. The strain gauges values measuring the bending moment as shown in Fig. 7 indicate clearly the stepwise changes in load; these also indicate, however, additional effects. The behaviour of the "clip gauge" for measuring the crack opening (fig. 8, above) is first comprehensible after 1600 s. The load steps are clearly recognisable after this point in time. Fig. 8, below, shows the temperature on the pipe outer surface directly adjacent to the crack. This temperature is clearly lower than that of the fluid in the pipe (see fig. 9, below). Both temperature distributions show the initial warming-up phase. Fig. 9, above, shows the measured leakrates (measuring procedures as in fig. 5) which - as for the CMOD - only show clear steps in the time after 1600 s; the maximum flow rate was 0,4 kg/sec.

4 CONCLUSIONS

All measurements generally reflect the incremental changes in measured values, resulting from the system being subject to a stepwise changing bending moment. In many cases an unexpected drift in values was detected, which is presumably due to temperature effects. Although the leak rates do not often exceed 0,5 kg/sec, these can increase up to approx. 2 kg/sec for longer cracks (E22.05). The previous unsatisfactory CMOD measurements led to the development of a new type of clip gauge. Although this new clip gauge has not been exhaustively tested, it could meanwhile be applied successfully to these tests (E22.05, E22.12).

The measuring is accompanied by and compared with results from finite element calculations and simplified calculation procedures (crack opening and massflow) /Grebner 1991/. This series of tests will be extended in 1991 by further tests on nozzles and pipe elbows.

REFERENCES

Grebner, H., Hunger, H., Höfler, A. (1991). Pre- and Post-Calculations for Crack Opening and Leak Rate Experiments on Piping Components within the HDR Program. Proceedings of SMIRT 11, Tokyo, Paper G24/1.

King, A., Hunger, H. (1990). Investigation of flow behaviour through leaks in small-bore piping systems. Quick Look Report-Test Group E22 (Part I), PHDR Technical Report No 105-90 (in German).

Grebner, H., Höfler, H. (1990). Untersuchungen zum Lecköffnungs- und Ausströmverhalten an Geradrohren mit Umfangsrissen bei Innendruck- und Biegebelastung, Bericht GRS-A-1747, Gesellschaft für Reaktorsicherheit, Köln.

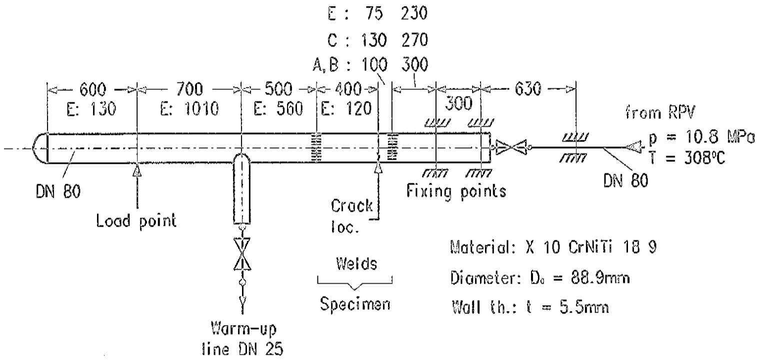

Fig. 1: Test pipes A, B, C, E for leak rate experiments E22.0i (schematically).

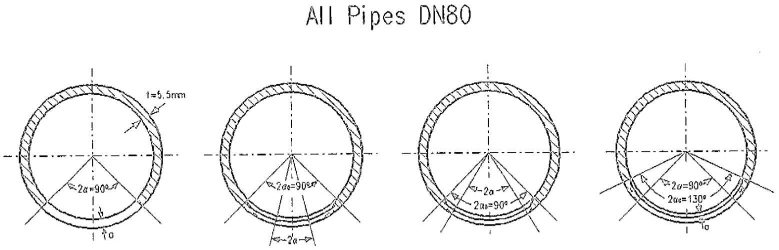

Slit a/t = 1 Slit width: 0.31mm (inside)	Notch a/t = 0.5 Notch width: 0.68mm Crack 2α = 28.4° (outs.) Crack width: 0.08mm (outside)	Notch a/t = 0.1 Crack I 2α = 50° Crack width: 0.22mm (outside) Crack II $2\alpha_i$ = 64.5°	Notch a/t = 0.5 Crack 2α = 90°
Pipe A (E22.01)	Pipe B (E22.02/03)	Pipe C (E22.04)	Pipe E (E22.05)

Fig. 2: Specimen with flaws for leak rate test series E22.0i.

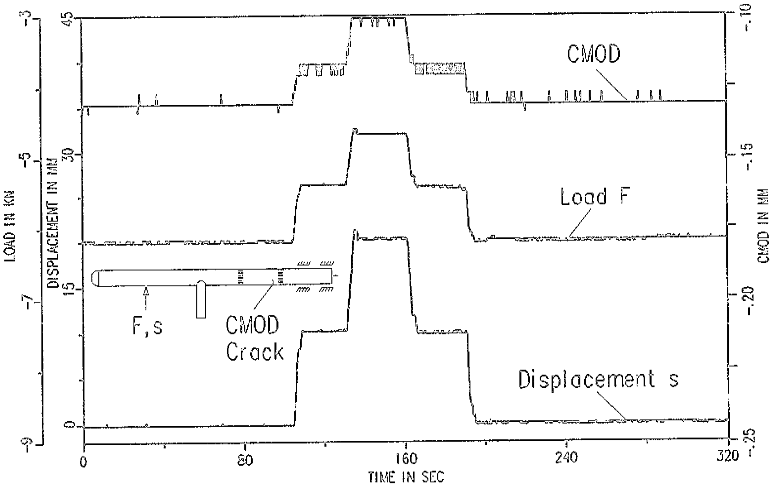

Fig. 3: "Cold" test E22.03 - Load and crack mouth opening displacement without temperature influence.

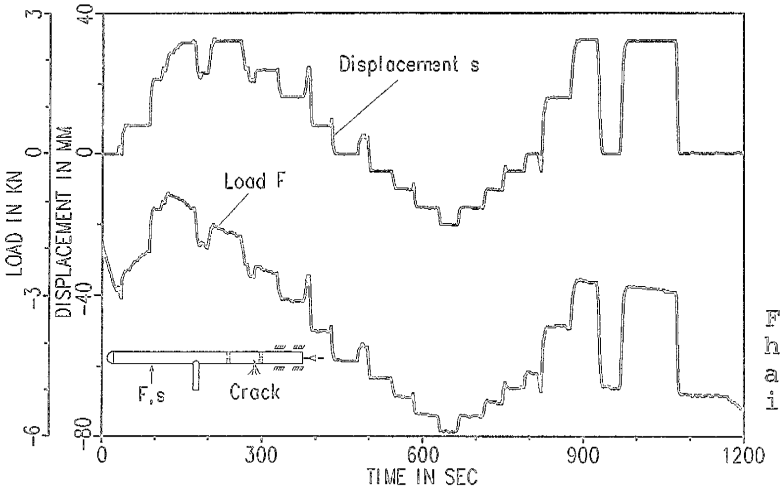

Fig. 4: Travel of hydraulic cylinder and resulting load in test E22.02

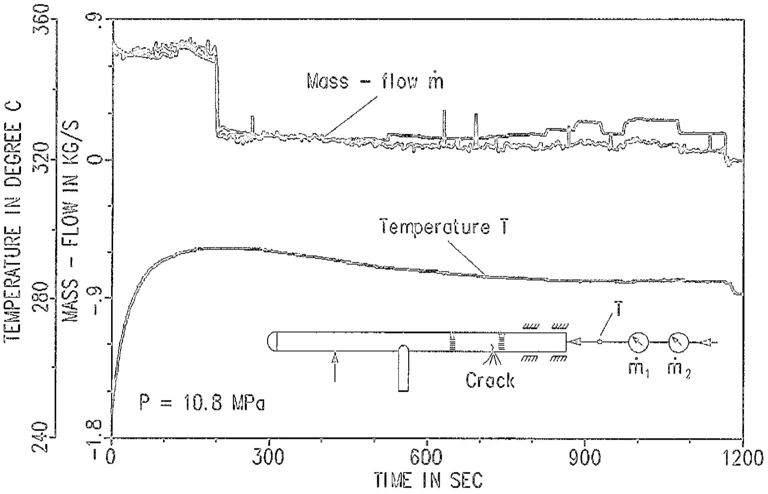

Fig. 5: Test E22. 02 - Temperature of fluid and mass-flow rate through crack (two different measuring methods)

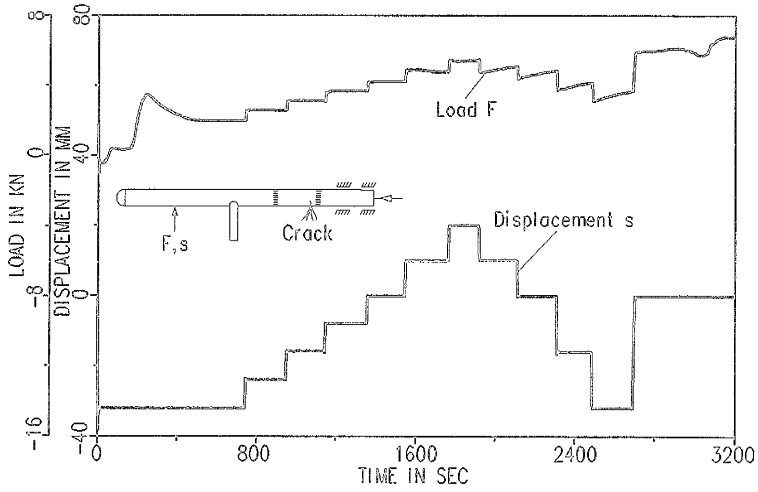

Fig. 6: Test E22. 04 - travel of hydraulic cylinder and resulting load

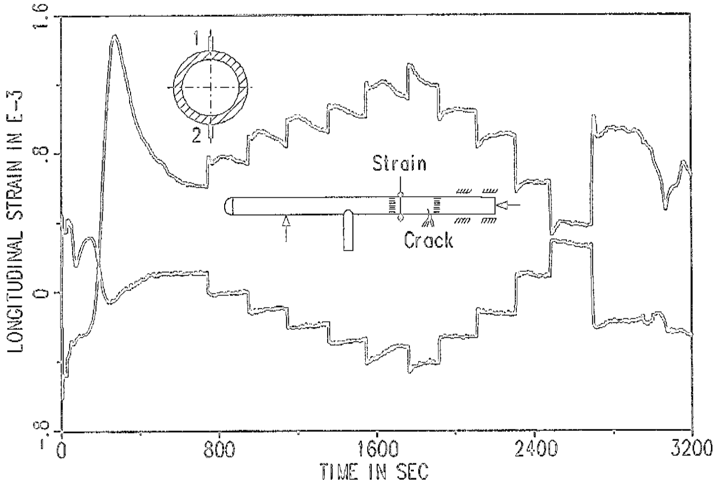

Fig. 7: Longitudinal strains near crack due to stepwise loading in test E22.04

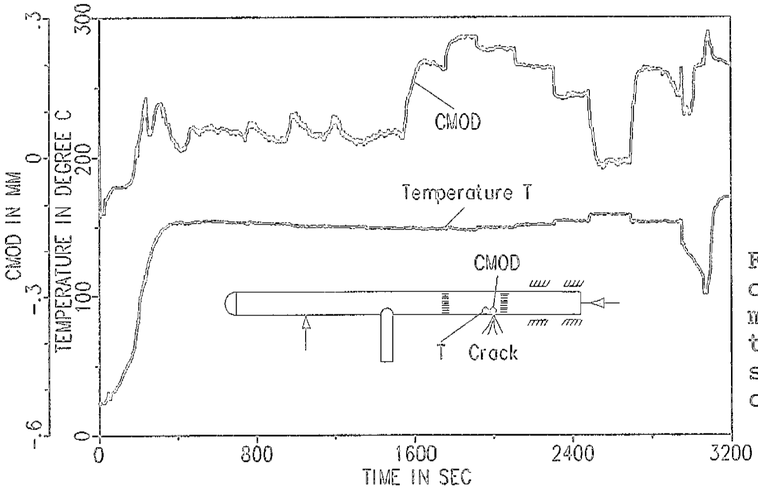

Fig. 8: Crack mouth opening displacement (CMOD) and temperature of outside wall close to crack in test E22.04

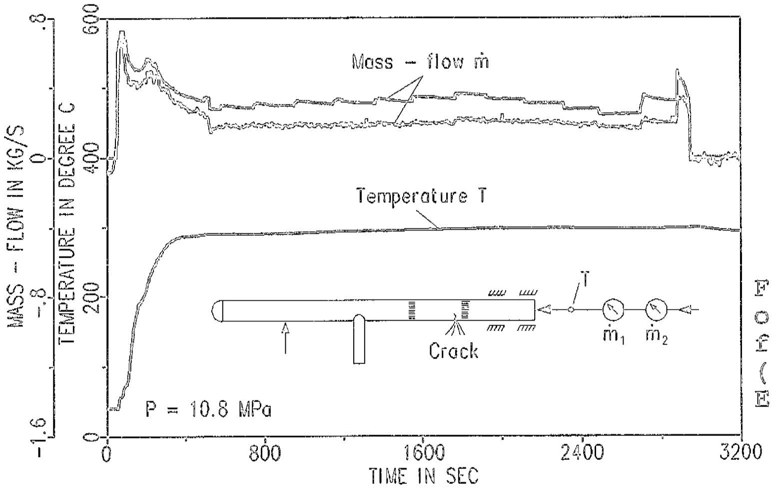

Fig. 9: Temperature of fluid and mass-flow through crack (2 methods) in test E22.04